

a slow protonation equilibrium of the metal complex,  $ML + H \rightleftharpoons MHL$ , and will suggest the drastic structural change from structure I to II. Under these conditions ( $C_M:C_L = 1:1$ ), some proportion of NTMP dissociates into free ligand. It was, however, confirmed by the studies of the solution containing an excess of the metal ion ( $C_M:C_L = 2:1$ ) that the dissociation of complex,  $ML' \rightleftharpoons M + L'$ , had little effect on the broadening of the signal. On the other hand, the sharp signals at lower pH (pH 7.8) indicate the fast protonation equilibria,  $MHL + H \rightleftharpoons MH_2L$  and  $MH_2L + H \rightleftharpoons MH_3L$ ; that is, the protonation of phosphonate ion is very fast.

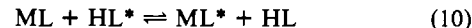
The  $^{31}P\{^1H\}$  NMR signal of the M-L solution at pH 7.8 shows a sharp single peak at any M:L ratio (Figure 4). As can be seen from the conditional formation constants (Figure 1B,C), 15-40% of the ligand in a  $C_M:C_L = 1:1$  solution does not form any complex. Thus, the chemical shift approaches the position of the  $ML'$  shift,  $\delta_{ML'}$ , on addition of excess of metal ion ( $C_M:C_L = 2:1$ ). When the M:L ratio is less than 1, the solution is a mixture of the complex  $ML'$  and the excess ligand  $L'$ . With decrease in the  $C_M:C_L$  ratio, the signal shifts to the position of the  $L'$  shift,  $\delta_{L'}$ . The signal appears at the position corresponding to the  $[ML']:[L']$  ratio. At this pH the predominant species are HL and MHL, and thus the predominant ligand exchange reaction is



The sharp  $^{31}P\{^1H\}$  signal indicates the fast ligand exchange of eq 9.

On the other hand, very broad signals were obtained for the solutions at pH 10.9 containing an excess ligand ( $C_M:C_L < 1$ ) and the signal of the Mg solution splits into two peaks. The signal of a Ba, Sr, or Ca solution appears at the position corresponding to the ratio of  $[ML']$  and  $[L']$ ; i.e., the plots of observed  $\delta_p$  as a function of  $C_M:C_L$  show straight lines in the range of  $C_M:C_L \leq 1$ . This fact supports the formation of M:L = 1:1 complexes

( $MH_mL$ ) under the conditions  $C_M:C_L \leq 1$ . The peaks for a Mg solution appear at the positions of  $ML'$  and  $L'$  signals. As the predominant species at pH 10.9 are HL and ML, the ligand exchange is written



The broadened signal indicates that this exchange reaction is relatively slow. The rate of exchange increases in the order  $Mg < Ca < Sr < Ba$ , which is the order of the ion size. Since in the case of the  $C_M:C_L = 1:1$  solution more than 90% of the total ligand exists in a single chemical form, unprotonated complex ML, the solution shows a sharp signal for ML. The fact that the  $^{31}P$  NMR shift is not constant at higher  $C_M:C_L$  ratios ( $C_M:C_L > 1$ ) may indicate the formation of polynuclear complexes such as  $M_2L$  under these conditions.

Thus, the  $^{31}P$  NMR data at various  $C_M:C_L$  ratios (Figure 4) indicate that the ligand exchange at pH 10.9 is much slower than at pH 7.8. As the difference of chemical shift between MHL and HL is much smaller than that between ML and HL and the contribution of the hydrogen ion concentration to the exchange rate was not studied, it is hard to discuss quantitatively the mechanism of ligand exchange. However, the results of line broadening suggest that the ligand exchange of the unprotonated species ML is slower than that of the protonated species MHL. This fact supports the structures proposed above; i.e., NTMP coordinates tightly to the alkaline-earth-metal ion as a tetradentate ligand in the ML complex (structure I) whereas it coordinates loosely by the ionic bond of three phosphonate ions in the MHL complex (structure II).

**Acknowledgment.** Financial support of this work from the Ministry of Education, Science, and Culture, Japan, is gratefully acknowledged. We thank Dr. K. Doi, Nagoya Institute of Technology, and Prof. T. Sotobayashi, Niigata University, for helpful discussions.

Contribution from the Chemistry Departments, University of Virginia, Charlottesville, Virginia 22901, and Dickinson College, Carlisle, Pennsylvania 17013

## Empirical Intensity Parameters for the 4f → 4f Absorption Spectra of Nine-Coordinate Erbium(III) Complexes in Aqueous Solution

Mark T. Devlin,<sup>†</sup> Eileen M. Stephens,<sup>†</sup> F. S. Richardson,<sup>\*†</sup> Thomas C. Van Cott,<sup>‡</sup> and Scott A. Davis<sup>‡</sup>

Received July 17, 1986

The Judd-Ofelt parametrization scheme for lanthanide 4f → 4f transition intensities is used to analyze absorption intensity data obtained for a series of Er(III) complexes in aqueous solution. Oscillator strengths are reported for eight multiplet-to-multiplet transition regions of each complex, and values for the Judd-Ofelt intensity parameters,  $\Omega_\lambda$  ( $\lambda = 2, 4, 6$ ), are determined and reported for each of the systems. Variations in the values of these parameters from system to system are discussed in terms of structural differences between the complexes (with respect to ligand properties and coordination geometry).

### Introduction

In a recent study<sup>1</sup> we reported absorption spectra, 4f → 4f oscillator strengths, and empirically determined 4f → 4f intensity parameters for a series of neodymium(III) and holmium(III) complexes in aqueous solution. The ligands included in that study were oxydiacetate (ODA), dipicolinate (DPA), iminodiacetate (IDA), (methylimino)diacetate (MIDA), and malate (MAL). The principal objectives were to characterize and compare the 4f → 4f absorption intensities observed for the various complexes, to obtain values for the Judd-Ofelt intensity parameters ( $\Omega_\lambda$ ) for each complex, and to relate variations in these parameters (among the different complexes) to differences in ligand structural properties.<sup>2</sup> In the present study, we report absorption spectra,

4f → 4f oscillator strengths, and Judd-Ofelt intensity parameters for a series of erbium(III) complexes in aqueous solution. The ligands included in this study are ODA, DPA, IDA, MIDA, and MAL, as well as chelidamate (CDA)<sup>3</sup> and chelidonate (CDO).<sup>4</sup> The objectives of this study are similar to those of our previously reported studies on neodymium(III) and holmium(III) complexes.<sup>1,2</sup>

(1) Stephens, E. M.; Davis, S. A.; Reid, M. F.; Richardson, F. S. *Inorg. Chem.* **1984**, *23*, 4607.

(2) Stephens, E. M.; Reid, M. F.; Richardson, F. S. *Inorg. Chem.* **1984**, *23*, 4611.

(3) Chelidamate (CDA) refers here to the deprotonated form of chelidamic acid (4-hydroxypyridine-2,6-dicarboxylic acid) in aqueous solution under alkaline pH conditions.

(4) Chelidonate (CDO) refers here to the deprotonated form of chelidonic acid (4-hydroxypyran-2,6-dicarboxylic acid) in aqueous solution under alkaline pH conditions.

<sup>†</sup> University of Virginia.

<sup>‡</sup> Dickinson College.

All of the results reported herein were obtained on aqueous solutions of  $\text{ErCl}_3$ -ligand in which the  $[\text{Er}]:[\text{ligand}]$  concentration ratio was 1:3 and the solution pH was in the range 8–10. Under these solution conditions, the major  $\text{Er}(\text{ODA})$  and  $\text{Er}(\text{DPA})$  species are undoubtedly tris(terdentate) complexes with effective  $D_3$  point-group symmetry.<sup>5,6</sup> It is likely that the major  $\text{Er}(\text{CDA})$  and  $\text{Er}(\text{CDO})$  species are also tris(terdentate) complexes with effective  $D_3$  symmetry.<sup>7</sup> The major  $\text{Er}(\text{IDA})$  and  $\text{Er}(\text{MIDA})$  species are likely to be tris(terdentate) complexes, but with an effective  $C_{3h}$  point-group symmetry.<sup>5,8</sup> It is difficult to even speculate about the major structural forms of  $\text{Er}(\text{MAL})$  complexes present in aqueous solution under alkaline pH conditions, although there is some evidence that the analogous  $\text{Tb}(\text{MAL})$  complexes are nine-coordinate with the hydroxyl groups of the malate ligands acting as donor moieties (along with the carboxylate groups).<sup>9</sup>

Each of the structures suggested above for the major species of the ODA, DPA, CDA, CDO, IDA, and MIDA complexes has ninefold coordination to the erbium ion; each has an  $\text{ErL}_6\text{L}'_3$  coordination polyhedron in which the L donor atoms are situated at the vertices of a trigonal prism (regular or slightly distorted) and the L' donor atoms occupy "capping" positions on normals to the rectangular faces of the prism; in each structure, the L donor atoms are carboxylate oxygens. The major differences in the structures are found in (1) the nature of the L' donor atoms (or groups), (2) the spatial dispositions of the chelate rings, and (3) the constituent and substituent atoms and bonds of the chelate rings. The L' donor atoms of the different ligands are either oxygen (ODA), pyridyl nitrogen (DPA and CDA), pyran oxygen (CDO), and amino nitrogen (IDA and MIDA). The only difference between IDA and MIDA is the H vs.  $\text{CH}_3$  substituent on the nitrogen donor atom, and CDA differs from DPA only by the presence of a 4-oxo substituent on the pyridyl group (in CDA). In the tris(terdentate) complexes of ODA, DPA, CDA, and CDO, the chelate rings are presumed to be planar and they stretch diagonally across the rectangular faces of the  $\text{ErL}_6\text{L}'_3$  tricapped trigonal prism, forming so-called meridional (or *mer*) isomeric structures of  $D_3$  symmetry.<sup>2,10</sup> On the other hand, in the tris(terdentate) complexes of IDA and MIDA, the chelate rings cannot be planar and the ligands are presumed to be wrapped around the  $\text{ErL}_6\text{L}'_3$  prism in a facial (or *fac*) configuration that has  $C_{3h}$  symmetry.<sup>2,10</sup> Finally, we note that whereas the tris complexes of ODA, DPA, IDA, and MIDA will have a net charge of -3, the tris complexes of CDA and CDO will have a net charge of -6 (under the solution conditions employed in this study).

Assuming that the structures described above provide reasonably accurate representations of the major species present in solution, one should be able to rationalize any observed variations in  $4f \rightarrow 4f$  intensity properties among the various complexes in terms of rather well-defined structural differences. Except for  $\text{Er}(\text{MAL})$ , each complex has an  $\text{ErL}_6\text{L}'_3$  coordination polyhedron with a tricapped trigonal prism structure, and the L donor atoms are the same in all the complexes. Structural differences occur primarily in the L' donor atoms (or groups), the configurational arrangement of chelate rings, and the chelate ring constituents and substituents (including both atoms and chemical bonds). Clearly, these complexes are good model systems for examining the more subtle aspects of intensity-structure correlations in lanthanide  $4f \rightarrow 4f$  spectra. Of course, some caution should be exercised in any attempt to rationalize observed intensity variations *entirely* in terms of the structures described above. Among the systems examined in this study, there are likely to be variations in the distributions of majority species and minority species present in solution, and these variations may contribute to differences in the  $4f \rightarrow 4f$  intensity properties.

**Table I.** Transition Regions and  $U^{\lambda}$  Matrix Elements Used in the Intensity Analyses

label	transition <sup>a</sup>	approx $\bar{\nu}_{\text{max}}/\text{cm}^{-1}$ <sup>b</sup>	$\langle U^{\lambda} \rangle^2$		
			$\lambda = 2$	$\lambda = 4$	$\lambda = 6$
Er(a)	$^4I_{15/2} \rightarrow ^4F_{9/2}$	15 250	0	0.5484	0.4616
Er(b)	$^4I_{15/2} \rightarrow ^4S_{3/2}$	18 350	0	0	0.2222
Er(c)	$^4I_{15/2} \rightarrow ^2H_{11/2}$	19 200	0.7254	0.4190	0.0939
Er(d)	$^4I_{15/2} \rightarrow ^4F_{7/2}$	20 500	0	0.1466	0.6259
Er(e)	$^4I_{15/2} \rightarrow ^4F_{5/2}$	22 150	0	0	0.2230
Er(f)	$^4I_{15/2} \rightarrow ^4F_{3/2}$	22 600	0	0	0.1257
Er(g)	$^4I_{15/2} \rightarrow ({}^2G, {}^2H, {}^4F)_{9/2}$	24 600	0	0.0203	0.2201
Er(h)	$^4I_{15/2} \rightarrow ^4G_{11/2}$	26 500	0.9042	0.5197	0.1173

<sup>a</sup> States are labeled according to their major SLJ component (or components). <sup>b</sup> The  $\bar{\nu}_{\text{max}}$  values observed for the absorption bands vary from system to system, so the values listed here are only meant to indicate the approximate locations of these bands.

### Experimental Section

$\text{ErCl}_3 \cdot 6\text{H}_2\text{O}$  (99.99%) was purchased from Aldrich and was used without further purification. Oxydiacetic acid, (methylimino)diacetic acid, chelidonic acid,<sup>4</sup> and malic acid were also purchased from Aldrich and used without further purification. Chelidamic acid<sup>3</sup> was purchased from Aldrich and was repurified twice, by using the procedure described by Bag et al.<sup>11</sup> Iminodiacetic acid and disodium dipicolinate were purchased from Sigma.

All spectroscopic measurements were carried out on aqueous solution samples in which  $[\text{Er}^{3+}] = 18 \text{ mM}$ . For  $\text{ErCl}_3$  in water, the solution pH was fixed at  $\sim 2$ . A concentration ratio of 1:3  $[\text{Er}^{3+}]:[\text{ligand}]$  was used for each of the ligand studies, with a solution pH  $\sim 8$ –10. Solution pH adjustments were made with  $\text{NH}_4\text{OH}$ . Absorption spectra were recorded on a Cary 17D spectrophotometer with the samples at room temperature. All absorption difference spectra were recorded with  $\text{ErCl}_3(\text{aq})$  in the reference beam and the  $\text{ErCl}_3$ -ligand-water system in the sample beam.

Absorption spectra were obtained over the  $14\,800$ – $27\,200\text{-cm}^{-1}$  energy region. This region contains eight multiplet-to-multiplet transitions originating from the  $^4I_{15/2}$  (ground) multiplet of  $\text{Er}(\text{III})$ . Oscillator strengths, defined here by

$$f = (4.32 \times 10^{-9}) \int \epsilon(\bar{\nu}) d\bar{\nu} \quad (1)$$

were determined for each of these transitions by evaluating  $\int \epsilon(\bar{\nu}) d\bar{\nu}$  over the transition region of interest. The eight transitions are identified according to their principal SLJ  $\rightarrow$  S'L'J' parentages in Table I.

### Intensity Parameter Calculations

According to the Judd-Ofelt theory of lanthanide  $4f \rightarrow 4f$  electric-dipole intensity,<sup>12-15</sup> the oscillator strengths of multiplet-to-multiplet transitions in a given system may be expressed as

$$f = (8\pi^2 m_e c / 3h) \chi \bar{\nu} (2J + 1)^{-1} \sum_{\lambda} \Omega_{\lambda} \langle \psi J || U^{\lambda} || \psi' J' \rangle^2 \quad (2)$$

where  $\psi J$  and  $\psi' J'$  label, respectively, the initial and final states of the  $\psi J \rightarrow \psi' J'$  multiplet-to-multiplet transition,  $\bar{\nu}$  is the energy of this transition (expressed in wavenumbers),  $\chi$  is the Lorentz field correction for the refractivity of the sample medium,  $2J + 1$  is the degeneracy of the  $\psi J$  electronic state,  $U^{\lambda}$  is an intraconfigurational unit-tensor operator,<sup>14</sup> and the  $\Omega_{\lambda}$  quantities ( $\lambda = 2, 4, 6$ ) are parameters that depend on the details of the lanthanide-ligand interactions and on the radial expectation values,  $\langle r^{-\lambda} \rangle$ , of the  $4f$  electrons. Expression 2 is applicable only to unpolarized spectra obtained on optically isotropic samples. Furthermore, it assumes that all the crystal field (or  $M_J$ ) sublevels of the initial ( $\psi J$ ) state are equally populated, and it neglects crystal field induced mixings between different multiplets. The  $U^{\lambda}$  matrix elements in eq 2 are evaluated between eigenstates of the  $4f^N$  electronic Hamiltonian in the intermediate-coupling approximation for the free ion.

For all of the transitions examined in this study, the initial multiplet state is  $^4I_{15/2}$ , and  $2J + 1 = 16$ . Assuming a fixed value of 1.19 for  $\chi$ , eq 2 may be evaluated to the form

$$f = (8.03 \times 10^9) \bar{\nu} \sum_{\lambda} \Omega_{\lambda} \langle \psi J || U^{\lambda} || \psi' J' \rangle^2 \quad (3)$$

in which  $\bar{\nu}$  is expressed in  $\text{cm}^{-1}$  and  $\Omega_{\lambda}$  is expressed in units of  $\text{cm}^2$ . The

- (5) Foster, D. R.; Richardson, F. S. *Inorg. Chem.* **1983**, *22*, 3996.  
 (6) Albin, M.; Whittle, R. R.; Horrocks, W. D. *Inorg. Chem.* **1985**, *24*, 4591.  
 (7) Pike, M. M.; Yarmush, D. M.; Balschi, J. A.; Lenkinski, R. E.; Springer, C. S. *Inorg. Chem.* **1983**, *22*, 2388.  
 (8) Salama, S.; Richardson, F. S. *J. Phys. Chem.* **1980**, *84*, 512.  
 (9) Salama, S.; Richardson, F. S. *Inorg. Chem.* **1980**, *19*, 629.  
 (10) Favas, M. C.; Kepert, D. L. *Prog. Inorg. Chem.* **1981**, *28*, 309.

- (11) Bag, S. P.; Fernando, Q.; Freiser, H. *Inorg. Chem.* **1962**, *1*, 887.  
 (12) Judd, B. R. *Phys. Rev.* **1962**, *127*, 750.  
 (13) Ofelt, G. S. *J. Chem. Phys.* **1962**, *37*, 511.  
 (14) Wybourne, B. G. *Spectroscopic Properties of Rare Earths*; Interscience: New York, 1965.  
 (15) Peacock, R. D. *Struct. Bonding (Berlin)* **1975**, *22*, 83.

**Table II.** Major SL Components of Multiplets Included in the Intensity Analyses

multiplet label <sup>a</sup>	energy/cm <sup>-1</sup> <sup>b</sup>	major SL components <sup>b</sup>
<sup>4</sup> I <sub>15/2</sub>	0	0.98 <sup>4</sup> I
<sup>4</sup> F <sub>9/2</sub>	15 191	-0.76 <sup>4</sup> F - 0.52 <sup>4</sup> I
<sup>4</sup> S <sub>3/2</sub>	18 304	0.83 <sup>4</sup> S - 0.44 <sup>2</sup> P
<sup>2</sup> H <sub>11/2</sub>	19 061	0.68 <sup>2</sup> H(1) + 0.60 <sup>4</sup> G - 0.39 <sup>4</sup> I
<sup>4</sup> F <sub>7/2</sub>	20 417	0.96 <sup>4</sup> F
<sup>4</sup> F <sub>5/2</sub>	22 091	-0.92 <sup>4</sup> F + 0.36 <sup>2</sup> D(1)
<sup>4</sup> F <sub>3/2</sub>	22 428	-0.79 <sup>4</sup> F + 0.46 <sup>2</sup> D(1) + 0.40 <sup>4</sup> S
( <sup>2</sup> G, <sup>2</sup> H, <sup>4</sup> F) <sub>9/2</sub>	24 481	-0.49 <sup>4</sup> F + 0.44 <sup>2</sup> G(2) - 0.40 <sup>2</sup> G(1) - 0.40 <sup>2</sup> H(1) + 0.35 <sup>4</sup> I + 0.26 <sup>2</sup> H(2)
<sup>4</sup> G <sub>11/2</sub>	26 301	0.77 <sup>4</sup> G - 0.52 <sup>2</sup> H(1) + 0.32 <sup>2</sup> H(2)

<sup>a</sup>These labels are identical with those used in Table I to identify multiplet-to-multiplet transition regions. <sup>b</sup>From calculations based on the free-ion Hamiltonian parameters listed in Table 5 (fourth column) of ref 16. The complete SLJ basis set for the 4f<sup>11</sup> electronic configuration was used in these calculations.

$U^{\lambda}$  matrix elements were evaluated in this study by using eigenvectors obtained by diagonalizing a 19-parameter Hamiltonian in the complete SLJ basis set for the 4f<sup>11</sup> electronic configuration of Er(III). The model Hamiltonian is that of Couture and Rajnak,<sup>16</sup> and the parameter values used in our calculations are those listed in Table 5 (the fourth column) of ref 16. The eigenvectors obtained from these calculations led to the  $\langle \psi || U^{\lambda} || \psi' \rangle^2$  values listed in Table I of the present paper. The major SLJ components of the relevant eigenvectors are given in Table II.

When empirically determined values for  $\bar{\nu}$  and  $f$  are inserted into eq 3, along with our calculated values for  $\langle \psi || U^{\lambda} || \psi' \rangle^2$ , the only unknown quantities in this equation are the  $\Omega_{\lambda}$  parameters (which, following common practice, we shall refer to as the Judd-Ofelt intensity parameters).<sup>15</sup> However, values for the  $\Omega_{\lambda}$  parameters may be obtained by a linear least-squares fitting procedure in which the  $\Omega_{\lambda}$  quantities ( $\lambda = 2, 4,$  and  $6$ ) are treated as adjustable parameters in fitting the empirically determined oscillator strengths for all eight transition regions listed in Table I to eq 3. The  $\Omega_{\lambda}$  values yielding optimal fits in this procedure are what we refer to as the "empirical intensity parameters". These parameters require no assumptions regarding 4f → 4f electric-dipole intensity theory (or mechanism) except for those inherent to eq 2.<sup>12-15,17,18</sup> Their detailed interpretation (or rationalization), on the other hand, requires explicit consideration of lanthanide-ligand-radiation field interaction mechanisms.<sup>2,17-20</sup>

## Results

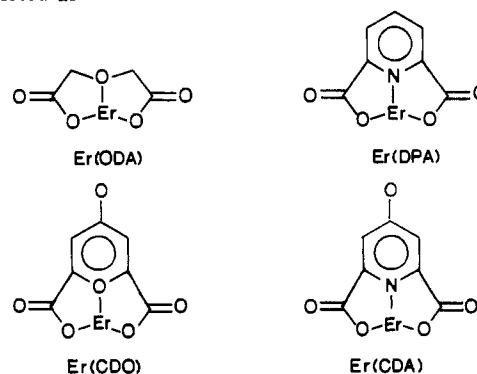
Experimental and fitted oscillator strengths are listed in Table III for each of the multiplet-to-multiplet transition regions examined in the present study. The "fitted" oscillator strengths were calculated from eq 3 by using empirical  $\bar{\nu}$  values, calculated  $\langle \psi || U^{\lambda} || \psi' \rangle^2$  values (given in Table I), and the  $\Omega_{\lambda}$  values given in Table IV. Ratios of  $\Omega_{\lambda}(\text{complex})/\Omega_{\lambda}(\text{aquo})$  are given in Table V.

Among the transition regions examined in this study, those labeled as Er(c) and Er(h) exhibit the largest variations in oscillator strength from complex to complex (see Table III). These regions are assigned to multiplet-multiplet transitions having predominantly <sup>4</sup>I<sub>15/2</sub> → <sup>2</sup>H<sub>11/2</sub> and <sup>4</sup>G<sub>11/2</sub> character (see Tables I and II). Among the  $\Omega_{\lambda}$  intensity parameters,  $\Omega_2$  exhibits the greatest sensitivity to the ligand environment (see Tables IV and V). The ligands most effective in producing 4f → 4f absorption intensity are CDO and CDA (see Tables III and IV). We note that quantitative intensity data could not be obtained for the Er(CDO) and Er(CDA) systems in the Er(h) (<sup>4</sup>I<sub>15/2</sub> → <sup>4</sup>G<sub>11/2</sub>) transition region due to the onset of a broad, and very intense, ligand absorption band in this region. The tail of this ligand absorption band overlays and obscures the much weaker <sup>4</sup>I<sub>15/2</sub> → <sup>4</sup>G<sub>11/2</sub> absorption band.

## Discussion

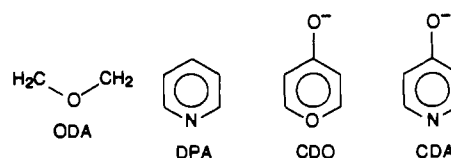
The results of primary interest in this study are those given in Tables IV and V. Clearly, the relative abilities of the various ligands to induce electric-dipole intensity in the 4f → 4f transitions are reflected primarily in the  $\Omega_2$  parameter values. This is not a novel finding. It has been recognized for many years that  $\Omega_2$  is the key parameter for making correlations between 4f → 4f (multiplet-multiplet) spectral intensities and ligand field properties.<sup>15,21-24</sup> Furthermore, given the sensitivity of  $\Omega_2$  to the ligand environment, it is clear why transitions with large  $U^2$  matrix elements should exhibit intensities that are hypersensitive to the ligand environment (see eq 2). The <sup>4</sup>I<sub>15/2</sub> → <sup>2</sup>H<sub>11/2</sub> and <sup>4</sup>G<sub>11/2</sub> transitions of Er(III) exhibit this hypersensitivity intensity behavior.

Except for Er(aquo), it is likely that the majority species present in solution for all of the systems listed in Table IV are nine-coordinate. For Er(aquo), the majority species are likely to be eight-coordinate Er(H<sub>2</sub>O)<sub>8</sub><sup>3+</sup> complexes with a square-antiprism structure of "effective"  $D_{4d}$  symmetry.<sup>16</sup> Perhaps the most interesting comparisons can be made among the Er(ODA), Er(DPA), Er(CDO), and Er(CDA) systems, each of which has majority species that are tris(terdentate) with trigonal dihedral ( $D_3$ ) symmetry. The individual chelate rings of these systems may be depicted as



In each case the chelate ring is expected to be planar, and in the tris complexes these chelate rings stretch diagonally across the rectangular faces of a tricapped trigonal prism formed by the coordinated (donor) atoms of the ligands. The tris complexes of Er(ODA) and Er(DPA) each have a net formal charge of -3, but under the solution conditions employed in our study, the tris complexes of Er(CDO) and Er(CDA) will each have a net charge of -6.

The relative values of the  $\Omega_2$  parameters listed in Table IV for the Er(ODA), Er(DPA), Er(CDO), and Er(CDA) systems may be expressed as 1.0 (ODA):1.5 (DPA):2.0 (CDO):2.3 (CDA). Assuming that tris(terdentate) complexes are the dominant species present in solution for each system, these differences in  $\Omega_2$  values may be ascribed primarily to differences in the equatorial binding moieties of the respective ligands. The axial binding moieties are chemically identical for the various systems (they are all carboxylate groups). Although the Er<sup>3+</sup>-carboxylate interactive strengths may be different in the various complexes, it is unlikely that these differences will affect the 4f → 4f transition intensities significantly.<sup>25</sup> The (extended) equatorial binding moieties of the various ligands are



- (16) Couture, L.; Rajnak, K. *Chem. Phys.* **1984**, *85*, 315.  
 (17) Reid, M. F.; Richardson, F. S. *J. Chem. Phys.* **1983**, *79*, 5735.  
 (18) Reid, M. F.; Richardson, F. S. *J. Phys. Chem.* **1984**, *88*, 3579.  
 (19) Dallara, J. J.; Reid, M. F.; Richardson, F. S. *J. Phys. Chem.* **1984**, *88*, 3587.  
 (20) Reid, M. F.; Richardson, F. S. *J. Chem. Phys.* **1984**, *80*, 3507.

- (21) Henrie, D. E.; Fellows, R. L.; Choppin, G. R. *Coord. Chem. Rev.* **1976**, *18*, 199.  
 (22) Mason, S. F. *Struct. Bonding (Berlin)* **1980**, *39*, 43.  
 (23) Judd, B. R. *J. Chem. Phys.* **1979**, *70*, 4830.  
 (24) Jørgensen, C. K.; Judd, B. R. *Mol. Phys.* **1964**, *8*, 281.  
 (25) Devlin, M. T.; Stephens, E. M.; Reid, M. F.; Richardson, F. S. *Inorg. Chem.*, following paper in this issue.

Table III. Experimental and Fitted Oscillator Strengths<sup>a</sup>

transition region <sup>b</sup>	complexes							
	aquo		ODA		DPA		CDO	
	exptl	fit	exptl	fit	exptl	fit	exptl	fit
Er(a)	2.66	2.44	2.80	2.94	2.99	2.99	3.53	3.35
Er(b)	1.19	0.73	1.07	1.06	1.32	1.08	1.50	1.19
Er(c)	3.13	3.75	6.50	7.37	9.22	10.40	13.92	13.65
Er(d)	2.75	2.66	3.42	3.75	3.52	3.76	4.25	4.08
Er(e)	1.11	0.88	0.97	1.30	1.19	1.30	1.26	1.37
Er(f)	0.44	0.50	0.36	0.75	0.59	0.72	0.96	0.89
Er(g)	0.92	1.01	1.46	1.48	1.41	1.49	nd <sup>c</sup>	1.59
Er(h)	7.19	6.54	13.52	12.85	19.03	17.84	nd <sup>c</sup>	23.42

	complexes							
	CDA		IDA		MIDA		MAL	
	exptl	fit	exptl	fit	exptl	fit	exptl	fit
Er(a)	3.74	3.78	3.06	2.88	2.92	3.02	2.50	2.55
Er(b)	1.16	1.19	1.32	0.89	0.85	0.96	0.61	0.71
Er(c)	15.91	15.85	7.08	7.80	8.62	9.76	5.15	5.86
Er(d)	4.29	4.34	3.09	3.08	3.22	3.51	2.51	2.72
Er(e)	1.24	1.42	1.20	1.11	1.11	1.17	0.87	0.87
Er(f)	0.87	0.83	0.68	0.63	0.60	0.67	0.36	0.50
Er(g)	1.26	1.58	1.26	1.16	1.23	1.36	0.99	1.04
Er(h)	nd <sup>c</sup>	27.11	14.72	13.48	17.91	16.94	10.90	10.24

<sup>a</sup> Values given as  $f/10^{-6}$ . <sup>b</sup> See Table I. <sup>c</sup> Values not determined.

Table IV. Intensity Parameters Obtained from Data Fits<sup>a</sup>

system <sup>b</sup>	$\Omega_\lambda/10^{-20} \text{ cm}^2$		
	$\lambda = 2$	$\lambda = 4$	$\lambda = 6$
	Er(aquo)	$2.03 \pm 0.29$	$1.90 \pm 0.39$
Er(ODA)	$5.26 \pm 0.48$	$1.61 \pm 0.64$	$3.23 \pm 0.74$
Er(DPA)	$7.81 \pm 0.69$	$1.67 \pm 0.92$	$3.23 \pm 1.05$
Er(CDO)	$10.45 \pm 0.26$	$2.06 \pm 0.29$	$3.41 \pm 0.34$
Er(CDA)	$12.03 \pm 0.18$	$2.55 \pm 0.20$	$3.56 \pm 0.23$
Er(IDA)	$5.33 \pm 0.77$	$2.17 \pm 1.03$	$2.44 \pm 1.18$
Er(MIDA)	$7.20 \pm 0.88$	$1.99 \pm 1.17$	$2.90 \pm 1.33$
Er(MAL)	$3.88 \pm 0.42$	$1.95 \pm 0.56$	$2.15 \pm 0.64$

<sup>a</sup> All values are given to within  $\pm 1\sigma$  as determined from the data-fitting procedure described in the text. <sup>b</sup> Er(aquo) refers to  $\text{ErCl}_3$  dissolved in water. All other systems refer to aqueous solutions of 1:3  $[\text{ErCl}_3]:[\text{ligand}]$  with pH 8–10.

Table V. Ratios of Intensity Parameters

ligand	$\Omega_\lambda(\text{complex})/\Omega_\lambda(\text{aquo})$		
	$\lambda = 2$	$\lambda = 4$	$\lambda = 6$
	ODA	2.59	0.85
DPA	3.85	0.88	1.51
CDO	5.15	1.08	1.59
CDA	5.93	1.34	1.66
IDA	2.63	1.14	1.14
MIDA	3.55	1.05	1.35
MAL	1.91	1.03	1.00

These moieties differ with respect to their valence-shell electron densities (and distributions) and the relative polarizabilities of their electronic distributions. The CDO and CDA ligands present the greatest (and most polarizable) electronic charge densities to the lanthanide ion, ODA presents the least, and DPA is somewhere in between. This ordering correlates with the relative values determined for the  $\Omega_2$  intensity parameters for the four Er(ligand) systems.

The tris(terdentate) complexes of IDA and MIDA have a symmetry ( $C_{3h}$ ) different from that ( $D_3$ ) of the analogous ODA, DPA, CDO, and CDA complexes.<sup>5,8</sup> Structurally,  $\text{Er}(\text{IDA})_3^{3-}$  and  $\text{Er}(\text{MIDA})_3^{3-}$  are expected to be identical *except* for the replacement of  $>\text{N}-\text{H}$  equatorial donor moieties with  $>\text{N}-\text{CH}_3$  moieties. Since the latter would present the greatest (and most polarizable) electronic charge density to the lanthanide ion, one might expect a larger  $\Omega_2$  value for  $\text{Er}(\text{MIDA})$  than for  $\text{Er}(\text{IDA})$ . From Table IV we see the  $\Omega_2(\text{MIDA})/\Omega_2(\text{IDA}) \cong 1.35$ .

We point out again that the  $\Omega_\lambda$  (Judd–Ofelt) parametrization of lanthanide  $4f \rightarrow 4f$  (multiplet-to-multiplet) electric-dipole transition intensities is independent of mechanistic considerations (except for the one-electron, one-photon approximation).<sup>17,18</sup> However, rationalization of  $\Omega_\lambda$  variations (as a function of ligand field geometry and ligand properties) generally requires explicit consideration of lanthanide–ligand–radiation field interaction mechanisms.<sup>2,17–19</sup> Mechanistic interpretations of the  $\Omega_\lambda$  parameters fall outside the scope of the present study, but they will be the subject of a subsequent study.<sup>25</sup> Suffice it to say here that the  $\Omega_2$  parameters are quite sensitive to relatively minor changes in the ligand environment of the lanthanide ions, whereas the  $\Omega_4$  and  $\Omega_6$  parameters are relatively insensitive to such changes. Among most of the systems examined in this study, differences in ligand coordination and structural properties occur only in the equatorial binding moieties (as they are defined in tris(terdentate) complexes with tricapped-trigonal-prism coordination polyhedra). However, even these small differences in ligand field properties produce significant variations in the  $\Omega_2$  parameter (see Tables IV and V) and in the oscillator strengths of transitions with strong  $|\Delta J| = 2$  character (see Tables I and III). Both the  $^4\text{I}_{15/2} \rightarrow ^2\text{H}_{11/2}$  and  $^4\text{I}_{15/2} \rightarrow ^4\text{G}_{11/2}$  transitions exhibit large intensity variations among the systems examined in this study.

**Acknowledgment.** This work was supported by the National Science Foundation (NSF Grant CHE-8215815 to F.S.R.).